Materials Science-Poland, *Vol. 26*, *No. 3*, *2008*

Influence of nickel ions on dielectric and other physical properties of $PbO–MoO_3–B_2O_3$ glass system

P. SYAM PRASAD, V. RAVI KUMAR, G. NAGA RAJU, N. VEERAIAH*

Department of Physics, Acharya Nagarjuna University P.G. Centre, Nuzvid-521 201, A.P. India

$PbO–MoO_3–B_2O_3$ glasses containing various proportions of NiO (ranging from 0 to 1.0 mol %) have been prepared. A number of methods viz., differential thermal analysis, spectroscopic (IR and UV-Vis optical absorption, and ESR spectra) and dielectric properties (ε', $\tan\delta$, a.c. conductivity σ_{ac} over a range of frequencies and temperatures) of these glasses has been employed in studies. The results of differential thermal analysis suggest a high glass forming ability for the glass containing 0.6 mol % of NiO. The studies of UV-Vis and IR spectra show that nickel ions occupy both tetrahedral and octahedral positions in the glass network with the dominance of the tetrahedral positions when the concentration of NiO is below 0.6 mol % in the glass matrix. The analysis of the results of studies of dielectric properties reveals that there is an increase in the rigidity and the dielectric breakdown strength of the glass when the concentration of NiO is around 0.6 mol %.

Key words: *$PbO–MoO_3–B_2O_3$ glass; Ni^{2+} ions; DTA pattern; dielectric properties; ESR spectra; optical absorption*

1. Introduction

Molybdenum borate based glasses have been the subject of many investigations due to their catalytic properties. Molybdenum ions inculcate high activity and selectivity in a series of oxidation reactions of practical importance in glass matrices [1, 2]. Molybdenum ions exists at least in two stable valence states, viz., Mo(V) and Mo(VI) in a glass network. They act both as network formers with MoO_4^{2-} structural units and alternate with BO_4 structural units; these ions may also act as modifiers depending upon their concentration and nature of the host network. ESR studies on the glasses containing molybdenum ions have identified the presence of octahedrally coordinated Mo(V) ions along with distorted octahedrons approaching tetragons. Further, Mo–O bond in molybdenum hexavalent oxide is identified as significantly covalent [3, 4].

*Corresponding author, e-mail: nvr8@redifmail.com

Results of a number of recent studies on various physical properties viz., spectroscopic, ionic conductivity, dielectric properties etc., of variety of glass systems containing molybdenum ions are available [5–13].

Divalent nickel ions are interesting paramagnetic ions to probe in glass systems. Nickel ions are reported to occupy both tetrahedral and octahedral positions in glass matrices. A number of recent studies on diversified inorganic glass systems containing Ni^{2+} ions are available [14–19]. Attempts have also been made to detect the lasing action of these ions in certain crystal and glass systems since they possess several strong absorption bands in the visible and NIR regions where the pumping sources are easily available [20]. Octahedrally positioned Ni^{2+} ions are expected to exhibit eye safe laser emission of wavelength 1.56 μm ($^3T_2 \rightarrow {}^3A_2$) even at room temperature with low threshold energy which is of great importance in telecommunication [21]. The concentrations of ions in tetrahedral or octahedral positions depend on the quantitative properties of modifiers and glass formers, size of the ions in the glass structure, their field strength, mobility of the modifier cation, etc. Further, the investigation on the coordinate chemistry of Ni^{2+} ions in molybdenum–borate glass network is of interest in itself, because these ions are expected to influence physical properties of the glasses to a large extent. Hence, it is felt worthwhile to throw some light on the structural aspects of $PbO–MoO_3–B_2O_3$ glasses containing small proportion of nickel ions by studying some of their physical properties viz., dielectric properties (the electric permittivity, ε', the loss, tanδ, a.c. conductivity σ_{ac}, in the frequency range 10^2–10^6 Hz and in the temperature range 30–300 °C and the dielectric breakdown strength in air), spectroscopic properties (optical absorption in IR and UV-Vis regions, and ESR).

2. Experimental

Within the glass forming region of $PbO–MoO_3–B_2O_3$ glass system, a particular composition $30PbO–4MoO_3–66B_2O_3$ is chosen for NiO doping in the present study. The details of the composition are:

N_0: $30PbO–4MoO_3–66.0B_2O_3$; N_2: $30PbO–4MoO_3–65.8B_2O_3$: 0.2NiO;

N_4: $30PbO–4MoO_3–65.6B_2O_3$: 0.4NiO; N_6: $30PbO–4MoO_3–65.4B_2O_3$: 0.6NiO;

N_8: $30PbO–4MoO_3–65.2B_2O_3$: 0.8NiO; N_{10}: $30PbO–4MoO_3–65.0B_2O_3$: 1.0NiO.

Appropriate amounts (all in mol %) of reagent grades of PbO, MoO_3, H_3BO_3 and NiO powders were thoroughly mixed in an agate mortar and melted in a thick-walled platinum crucible in the temperature range 950–1050 ºC in an automatic temperature controlled furnace for about 1 h until a bubble free transparent liquid was formed. The resultant melt was then poured in a brass mould and subsequently annealed from 300 °C with a cooling rate of 1 ºC/min. The amorphous state of the glasses was checked by X- ray diffraction.

The samples were then ground and optically polished. The final dimensions of the samples used for dielectric and optical studies were about $1\times1\times2$ cm^3. The densities *d*

of the glasses were determined to the accuracy of 0.001 by the standard principle of Archimedes using *o*-xylene (99.99% pure) as the buoyant liquid. Differential thermal analysis was carried out using STA 409C model DTA-TG instrument with a programmed heating rate of 10 °C/min, in the temperature range 30–1000 ºC to determine the glass transition temperature and other glass forming ability parameters. The optical absorption spectra of the glasses were recorded at room temperature in the wavelength range 350–1400 nm up to the resolution of 0.1 nm using Shimadzu UV Vis-NIR spectrophotometer model 3101. The ESR spectra of fine powders of the samples were recorded at room temperature on E11Z Varian X-band (ν = 9.5 GHz) ESR spectrometer. Infrared transmission spectra were recorded on a Bruker IFS 66 V – IR spectrophotometer with a resolution of 0.1 cm^{-1} in the range 400–2000 cm^{-1} using potassium bromide pellets (300 mg) containing pulverized glass (1.5 mg). These pellets were pressed in a vacuum die at ca. 680 MPa. A thin coating of silver paint was applied (to the larger area faces) on either side of the glasses to serve as electrodes for dielectric measurements. The painted samples were then dried with a hot blower for about 10 minutes on either side. The details of dielectric measurements were similar to those reported in earlier papers from our laboratory [22, 23].

3. Results

Based on the glass density d and calculated average molecular weight $\bar{M}$, various physical parameters such as nickel ion concentration N_i, mean nickel ion separation r_i are evaluated for understanding the physical properties of these glasses using the conventional formulae [24] and the values obtained are presented in Table 1.

Table 1. Physical parameters of $PbO–MoO_3–B_2O_3$ glasses doped with NiO

Glass	Density d [g/cm^3]	Average mol.wt. M	Total nickel ion concentration [10^{21} ions/cm^3]	Interionic distance of Ni ions r_i [Å]
N_0	4.650	118.66	–	-
N_2	4.665	118.67	4.735	5.95
N_4	4.676	118.68	9.495	4.72
N_6	4.682	118.69	14.25	4.12
N_8	4.695	118.70	19.057	3.74
N_{10}	4.702	118.71	23.85	3.47

Figure 1 shows typical differential thermal analysis traces of $PbO–MoO_3–B_2O_3$ glasses doped with NiO of various concentrations. The curves exhibit an endothermic effect due to glass transition temperature T_g; the value of T_g is evaluated from the point of inflection of this feature. At still higher temperatures an exothermic peak T_c due to the crystal growth followed by an endothermic effect due to the melting effect T_m are also observed. The values of T_g, T_c and T_m obtained for all the glasses are given in Table 2.

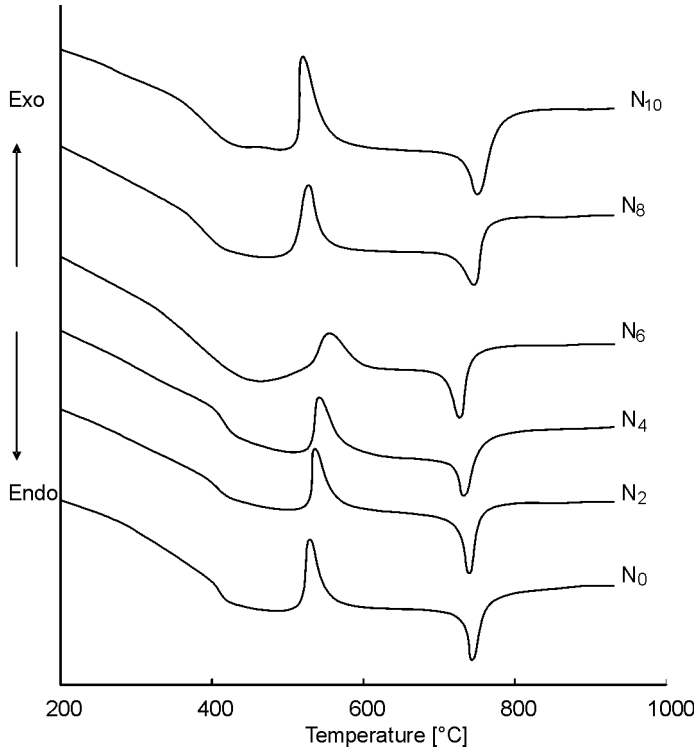

Fig. 1. DTA patterns of NiO-doped PbO–MoO_3–B_2O_3 glasses

Table 2. Results of differential thermal analysis of PbO–MoO_3–B_2O_3: NiO glasses

Glass	T_g	T_c	T_m	T_g/T_m	$(T_c-T_g)/T_g$	$(T_c-T_g)/T_m$	K_{gl}
N_0	701	802	1017	0.689	0.144	0.099	0.469
N_2	705	809	1013	0.695	0.147	0.102	0.509
N_4	710	814	1007	0.705	0.146	0.103	0.538
N_6	717	828	1001	0.716	0.154	0.110	0.641
N_8	697	800	1020	0.683	0.147	0.100	0.468
N_{10}	692	793	1025	0.675	0.145	0.098	0.435

The appearance of a single peak due to the glass transition temperature in DTA pattern of all the glasses indicates the homogeneity of the glasses prepared. Upon increasing concentration of NiO in the glass matrix, the difference $T_c - T_g$, which is proportional to glass forming ability, is found to increase whereas the difference $T_m - T_c$ which is inversely proportional to glass forming ability is found to decrease, with the increase in the concentration of NiO up to 0.6 mol %. From the measured values of T_g, T_c and T_m, the parameters T_g/T_m, $(T_c - T_g)/T_g$, $(T_c - T_g)/T_m$ and glass forming ability parameter K_{gl}, known as the Hruby parameter given by $(T_c - T_g)/(T_m - T_c)$, are evaluated; the value of these parameter exhibits maximum at $x \approx 0.6$ (Table 2, Fig. 2).

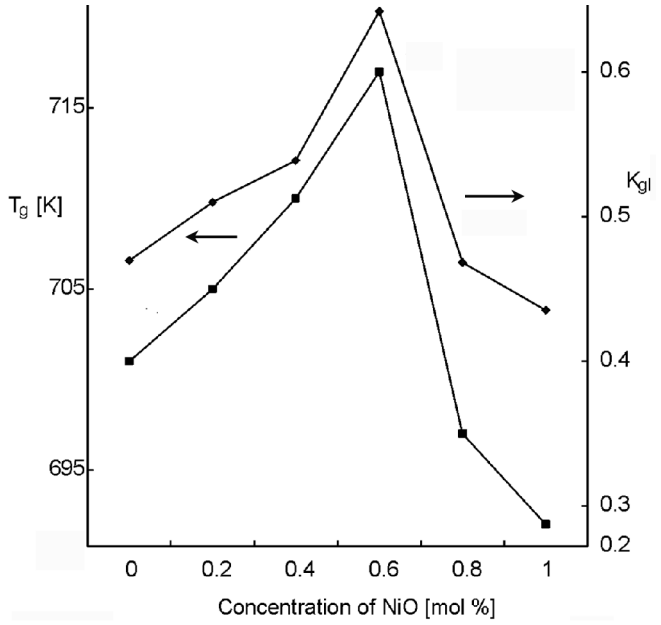

Fig. 2. Dependences of T_g and K_{gl} on the concentration of NiO

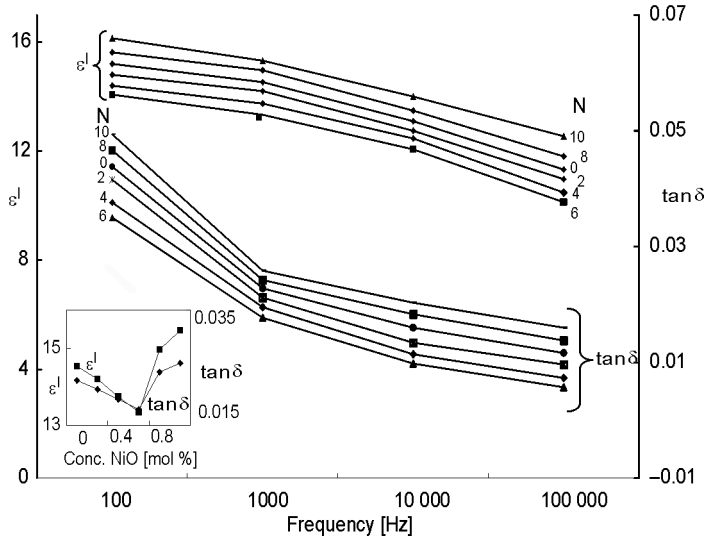

Fig. 3. Dependences of electric permittivity (ε^l) and loss (tanδ) on frequency at room temperature for $PbO–MoO_3–B_2O_3$ glass containing various amounts of NiO. The inset shows dependences of ε^l and tanδ on concentration of NiO at 1 kHz

The electric permittivity ε' and loss tanδ at room temperature (30 °C) of nickel free $PbO–MoO_3–B_2O_3$ glasses at 100 kHz are measured to be 11.32 and 0.0116, respectively; the values of ε' and tanδ are found to increase considerably upon decreasing

frequency (Fig. 3). The dependence of these parameters with the concentration of NiO showed a decreasing trend in the composition range $0 \leq x \leq 0.6$, whereas beyond 0.6 mol % the parameters were found to increase (inset of Fig. 3).

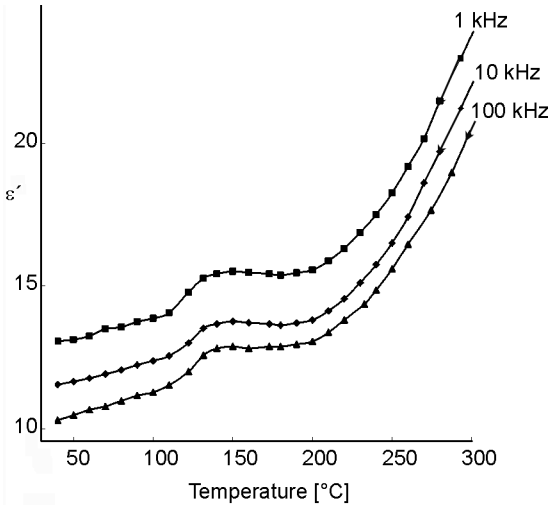

Fig. 4. Temperature dependences of electric permittivity of glass N_2 at various frequencies

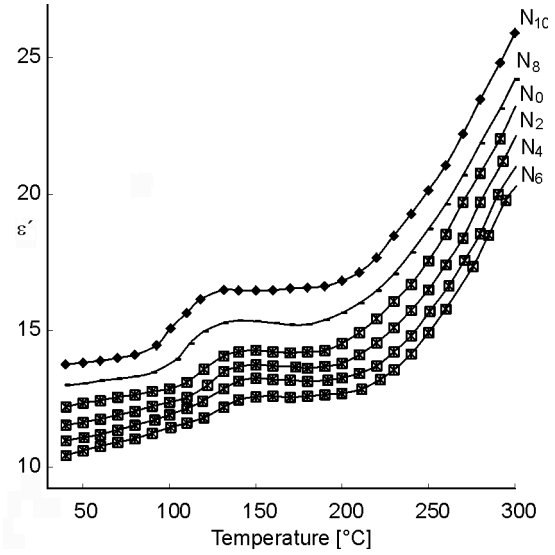

Fig. 5. Temperature dependences of electric permittivity at 10 kHz of $PbO–MoO_3–B_2O_3$ glasses doped with NiO of various concentrations

The temperature dependence of ε' at various frequencies of the glass N_2 (containing 0.2 mol % of NiO) and of the glasses containing various proportions of NiO at 10 kHz are shown in Figs. 4 and 5, respectively; the value of ε' is found to exhibit a con-

siderable increase at higher temperatures especially at lower frequencies for all the glasses maintaining the lowest value for glass N_6 at any frequency and temperature.

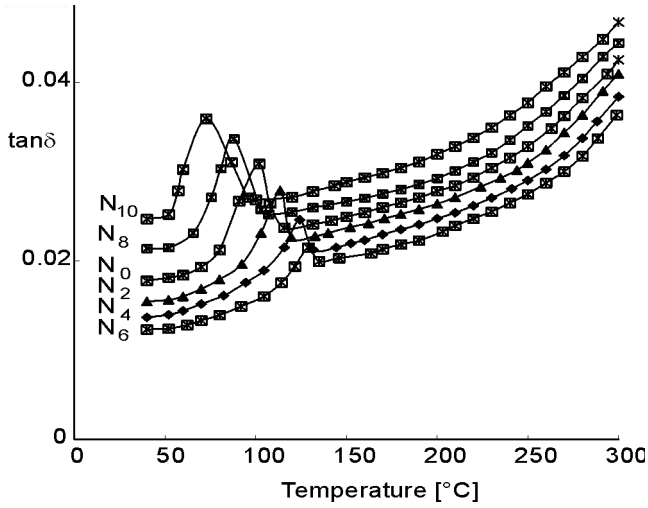

Fig. 6. Temperature dependences of dielectric losses at 1 kHz for PbO–MoO_3–B_2O_3 glasses doped with NiO of various concentrations

The temperature dependence of $\tan\delta$ of all the glasses at 1 kHz is presented in Fig. 6. The loss curve (of pure and NiO doped glasses) exhibited distinct maxima; upon increasing frequency, the temperature maximum shifts towards higher temperatures, and upon increasing temperature the frequency maximum shifts towards higher frequencies, indicating the relaxation character of dielectric losses of PbO–MoO_3 –B_2O_3: NiO glasses. The observations on dielectric loss variation with temperature for various concentrations of NiO further indicate a gradual increase in the broadness and $(\tan\delta)_{max}$ of relaxation curves beyond 0.6 mol % of NiO. The Cole–Cole diagrams drawn between ε' and ε'', corresponding to 120 °C in the relaxation region showed that the dielectric relaxation in these glasses is a Debye-type relaxation with a certain set of relaxation times τ. From these diagrams, low- and high-frequency electric permittivities (ε_s and ε_∞, respectively) have been determined for samples doped with various amounts of NiO. The obtained average values of ε_s and ε_∞ for each concentration are presented in Table 3.

Table 3. Data on dielectric loss of PbO–MoO_3–B_2O_3: NiO glasses.

Glass	$(\tan\delta)_{max}$	Temperature range of relaxation [°C]	ε_s	ε_∞	Activation energy for dipoles [eV]	α
N_2	0.027	79–108	12.2	5.8	1.81	7
N_4	0.024	84–106	10.8	5.35	1.99	5
N_6	0.021	88–104	10.2	5.15	2.20	3
N_8	0.032	80–109	16.8	9.6	1.92	9
N_{10}	0.036	74–114	17.9	11.7	1.88	10

The parameter α characterizing the distribution function τ does not show any considerable change with temperature for a particular concentration; however, for different concentrations, the values are appreciably different (Table 3). The effective activation energy W_d for the dipoles is calculated for different concentrations of NiO and presented also in Table 3. The activation energy is found to be the highest for glass N_6.

The a.c. conductivity σ_{ac} may be calculated at various temperatures from the equation:

$$\sigma_{ac} = \omega\varepsilon'\varepsilon_0 \tan\delta \tag{1}$$

where ε_0 is the vacuum electric permittivity for different frequencies. The dependences of $\log\sigma_{ac}$ on $1/T$ for all the glasses at 100 kHz are given in Fig. 7.

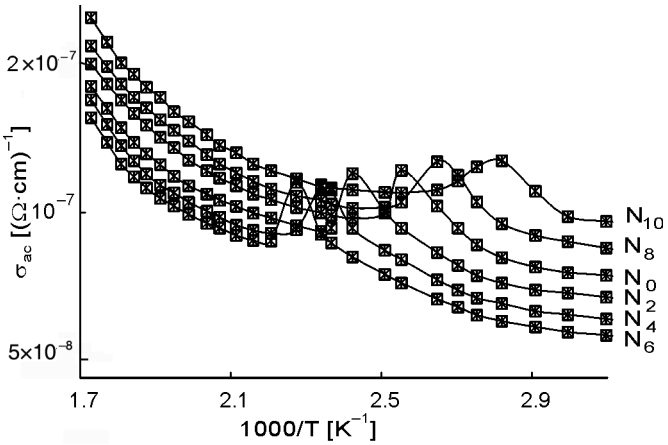

Fig. 7. Dependences of σ_{ac} on $1000/T$ for $PbO–MoO_3–B_2O_3$ glasses doped with NiO of various concentrations

Table 4. Data on a.c. conduction of $PbO–MoO_3–B_2O_3$: NiO glasses (See Sect. 4 for the discussion of $N(E_F)$)

Glass	$N(E_F)$ [$eV^{-1}\cdot cm^{-3}$]			Activation energy for conduction [eV]
	Austin and Mott [45]	Butcher and Hyden [51]	Pollak [52]	
N_2	8.91	3.72	9.06	0.251
N_4	8.33	3.47	8.46	0.265
N_6	7.77	3.24	7.90	0.284
N_8	10.50	4.38	10.7	0.258
N_{10}	11.40	4.75	11.6	0.248

The conductivity is found to decrease upon increasing concentration of NiO (at any given frequency and temperature) up to 0.6 mol % and beyond that it is found to increase. From these plots, the activation energy for conduction in the high tempera-

ture region over which a near linear dependence of $\log\sigma_{ac}$ on $1/T$ could be observed, is evaluated and presented in Table 4; activation energy is found to be the maximum for glass N_6 and minimum for glass N_{10}.

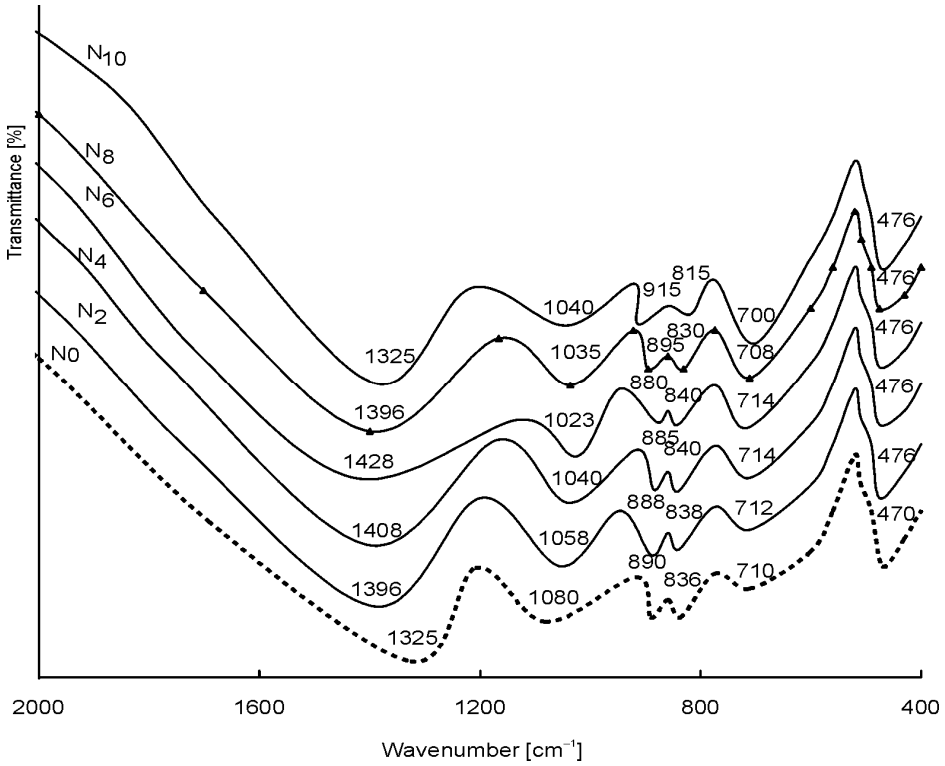

Fig. 8. IR spectra of PbO–MoO_3–B_2O_3: NiO glasses

The IR spectra of these glasses exhibited prominent bands in the regions 1300 –1400 cm^{-1}, 1000–1200 cm^{-1} and another band at about 710 cm^{-1} (Fig. 8); these bands are identified as due to the stretching relaxation of B–O bonds of the trigonal BO_3 units, vibrations of BO_4 structural units and due to the bending vibrations of B–O–B linkages, respectively [25]. Additionally, the band due to the vibrations of PbO_4 structural units is also located at about 470 cm^{-1} in the spectra of all the glasses. Yet, the spectra exhibit two well resolved bands at about 890 and 836 cm^{-1}; based on the earlier reported data [26, 27], these two bands have been attributed to ν_1 and ν_3 vibrational modes of MoO_4^{2-} tetrahedral units, respectively. Upon increase in the concentration of the dopant NiO, beyond 0.6 mol %, the following changes have been observed in the spectra: (i) the intensities of the bands due to MoO_4^{2-} tetrahedral units is observed to decrease and the band at 890 cm^{-1} is found to be shifted towards slightly higher frequency side whereas the band at 836 cm^{-1} is observed to be shifted towards

lower frequency (Table 5); (ii) the intensity of the band due to BO_3 structural units is observed to increase at the expense of the band due to BO_4 units.

Table 5. Band positions (in cm^{-1}) in the IR spectra of $PbO–MoO_3–B_2O_3$: NiO glasses

Glass	Borate groups			PbO_4	MoO_4 units	
	BO_3	BO_4	B–O–B			
N_0	1325	1080	710	470	890	836
N_2	1396	1058	712	476	888	838
N_4	1408	1040	714	476	885	840
N_6	1428	1023	714	476	880	840
N8	1400	1035	708	476	895	830
N_{10}	1389	1043	700	476	915	815

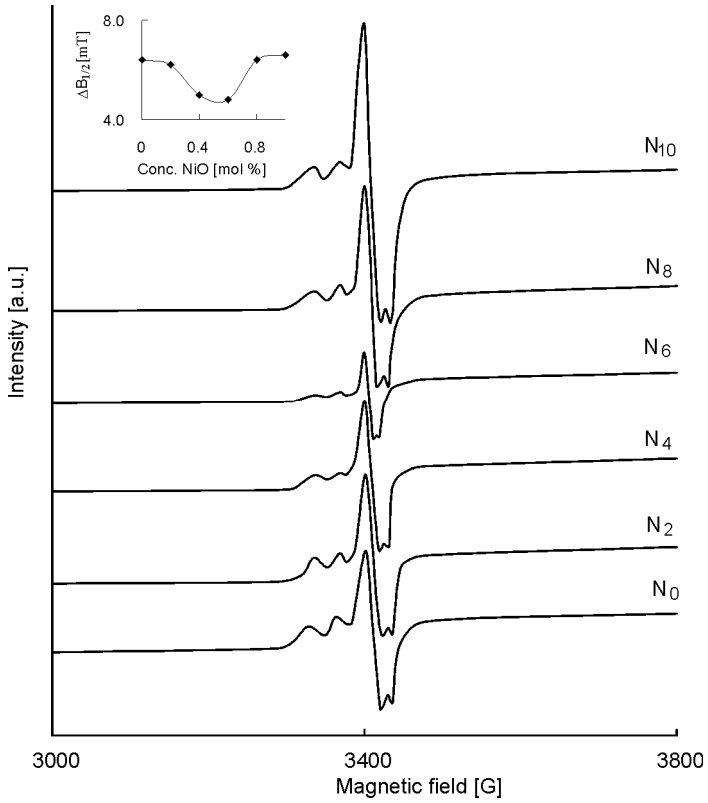

Fig. 9. ESR spectra of $PbO–MoO_3–B_2O_3$: NiO glasses recorded at room temperature; the inset gives the dependence of the half width $\Delta B_{1/3}$ on concentration of NiO

The ESR spectra (Fig. 9) of $PbO–MoO_3–B_2O_3$: NiO glasses recorded at room temperature exhibit a signal consisting of a central line surrounded by smaller satellites at about $g_\perp$ =1.943 and g_{ll} =1.886. The intensity and the half width $\Delta B_{1/2}$ of the central

line are observed to increase considerably when the concentration of NiO is increased beyond 0.6 mol % in the glass matrix (inset of Fig. 9).

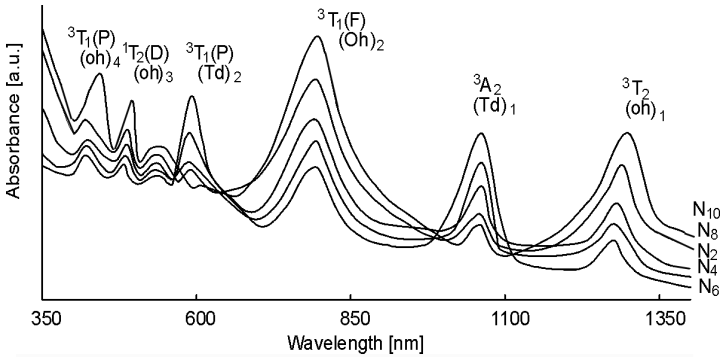

Fig. 10. Optical absorption spectra of PbO–MoO_3–B_2O_3: NiO glasses

The optical absorption spectra of PbO–MoO_3–B_2O_3: NiO glasses recorded at room temperature in the wavelength range 350–1400 nm are shown in Fig. 10. The spectrum of NiO free glasses exhibited an absorption band at about 550 nm (not shown in the figure). The intensity of this band is observed to be the largest in the spectrum of glass N_{10} and the lowest in the spectrum of glass N_6. Additionally, with the NiO doping the spectra exhibited several absorption bands due to Ni^{2+} ions. The spectrum of the glass (N_2) exhibited six clearly resolved intense absorption bands in the visible and NIR regions at 1282 nm (O_{h1}), 1061 nm (T_{d1}), 794 nm (O_{h2}), 590 nm (T_{d2}), 488 (O_{h3}) and at 422 nm (O_{h4}). As the concentration of NiO is increased up to 0.6 mol %, the intensity of the octahedral bands (O_h bands) is observed to decrease with a shift towards slightly lower wavelengths; in this concentration range the intensity of the two tetrahedral bands (T_d bands) is observed to increase with no considerable shift in the band positions. With the increase in the concentration of NiO from 0.6 to 1.0 mol %, the positions of the octahedral bands are shifted towards slightly higher wavelengths with increasing intensity at the expense of T_{d1} and T_{d2} bands. The summary of the data on the positions of various absorption bands is given in Table 6.

Table 6. Summary of the data on optical absorption spectra of NiO doped PbO–MoO_3–B_2O_3 glasses

Transition of nickel ions	Band positions [cm^{-1}]				
	N_2	N_4	N_6	N_8	N_{10}
Octahedral transitions					
$^3A_2$ (F) → $^3T_2$ (F)	7800	7824	7849	7745	7692
$^3A_2$ (F) → $^3T_1$ (F)	12589	12594	12666	12626	12562
$^3A_2$ (F) → $^1T_2$ (D)	20491	20618	20790	20491	20242
$^3A_2$ (F) → $^3T_1$ (P)	23640	23696	23809	23690	22376
Tetrahedral transitions					
$^3A_2$ (F) → $^3A_2$ (F)	9433	9433	9433	9433	9433
$^3A_2$ (F) → $^3T_1$ (F)	17543	17543	17543	17543	17543

4. Discussion

$PbO–B_2O_3$-MoO_3: NiO glasses have complex compositions being mixtures of network formers, intermediates and modifiers. It is a well known fact that B_2O_3 is a network former with BO_3 and BO_4 structural units. The presence of such BO_3 and BO_4 units in the $PbO–MoO_3–B_2O_3$: NiO glasses is evident from infrared spectral studies. PbO, which is $[PbO_{2/2}]$, tends to become four-connected to oxygens as $[PbO_{4/2}]^{2–}$ by acquiring this additional coordination. The band observed in the IR spectra at about 470 cm^{-1} suggests that there is a possibility for PbO to participate in the glass network with PbO_4 structural units. But at certain concentrations of PbO it also acts as a modifier. As a modifier, PbO enters the glass network by breaking up the B–O–B, B–O–Mo bonds (normally the oxygens of PbO break the local symmetry while Pb^{2+} ions occupy interstitial positions) and introduces coordinate defects known as dangling bonds along with non-bridging oxygen ions. In this case lead ions are octahedrally positioned. If NiO acts as a modifier in the glass network, additional non-bridging Pb–O bonds are expected to be formed at the expense of the bridging B–O–B and B–O–Pb linkages and may also introduce more non-bridging oxygen ions.

Molybdenum ions are expected to exist mainly in Mo^{6+} state in the $PbO–MoO_3–B_2O_3$ glass network; these ions are expected to participate in the glass network with tetrahedral $MoO_4^{2–}$ structural units and may alternate with BO_4 structural units. As the concentration NiO is increased (especially beyond 0.6 mol %), the colour of glasses becomes increasingly brown, indicating the reduction of molybdenum ions from Mo^{6+} state in to Mo^{5+} state. These Mo^{5+} (d^1) ions are quite stable and occupy octahedral positions with distortion due to the Jahn–Teller effect [28, 29].

The Ni^{2+} ions seem to exist in both four-fold and in six-fold coordination in the present glass network. In general, tetragonally positioned Ni^{2+} ions do not induce the formation of any non bridging oxygen ions but octahedrally positioned ions may act as modifiers [30].

Upon increasing concentration of NiO up to 0.6 mol %, the values of the glass transition temperature T_g and glass forming ability parameter K_{gl}, increase. The augmented cross-link density of various structural groups and closeness of packing are responsible for such an increase of these parameters. These results apparently suggest that there is a growing presence of tetrahedrally positioned nickel ions which increase the cross-link density and enhance the mean bond strength.

Using the Tanabe–Sugano diagrams for $Ni^{2+}(d^8)$ ion, the optical absorption spectra have been analyzed and the bands O_{h1}, O_{h2} and O_{h3} are assigned to the transitions from the $^3A_2$ ground state of octahedrally positioned Ni^{2+} ions to $^3T_2(F)$, $^3T_1(F)$ and $^3T_1(P)$ excited states, respectively. The bands with barycentres at about 1060 nm (T_d1) and 570 nm (T_d2) nm are attributed to the transitions $^3T_1(F) \rightarrow {}^3A_2(F)$ and $^3T_1(F) \rightarrow {}^3T_1(P)$ of Ni^{2+} ions in tetrahedral sites [31]; the band at about 420 nm represents a spin forbidden octahedral transition $^3A_2 \rightarrow {}^1T_2$ [21, 32]. Thus, the measurements of the optical absorption of $PbO–B_2O_3–MoO_3$: NiO glasses indicate that Ni^{2+} ions exist both in octa-

hedral and tetrahedral sites in the glass network. Further, the way the intensity of these bands varies with the concentration of NiO suggests that at smaller concentrations ($\leq$ 0.6 mol %), Ni^{2+} ions prefer to occupy tetrahedral positions whereas at larger concentrations, these ions occupy octahedral sites also in the glass network.

From these spectra it is also evident that the ratio, Ni^{2+}(oct)/Ni^{2+}(tet), increases with increase in the concentration of NiO beyond 0.6 mol %; further, the d–d transitions of the tetrahedral complexes are electric dipole allowed whereas those of octahedral complexes are electric dipole forbidden and are mainly due to static or dynamic distortions from the regular octahedral geometry of the glass network and they can also be magnetic dipole allowed.

Additional absorption band observed in the region 500–570 nm in the optical absorption spectra of these glasses is attributed to the excitation of Mo^{5+} ($4d^1$) ion [33]. In fact, for this ion, two optical excitations were predicted starting from b_2 (d_{xy}) ground state to ($d_{xz–yz}$) and ($d_{x^2-y^2}$) with δ = 15 000 cm^{-1} and Δ = 23 000 cm^{-1} [33]. Perhaps, due to intercharge transition transfer ($Mo^{5+} \longleftrightarrow Mo^{6+}$) in the glass network, the resolution of these transitions could not be observed. The highest intensity of this band observed in the spectrum of glass Mo_5 points out that the presence of the highest concentration of Mo^{5+} ions in these glasses. Such Mo^{5+} ions may form $Mo^{5+}O^{3-}$ molecular orbital states and are expected to participate in the depolymerisation of the glass network [33, 34] creating more bonding defects and non-bridging oxygens (NBO's) similar to octahedrally positioned Ni^{2+} ions.

The existence of molybdenum ions in Mo^{5+} state in these glasses is further confirmed by ESR spectral studies. The ESR spectrum of these glasses consists of a main central line surrounded by less intense satellites. The central line arises from even molybdenum isotopes (I = 0) whereas satellite lines correspond to the hyperfine structure from odd ^{95}Mo and ^{97}Mo (I = 5/2) isotopes [35]. The intensity of the signal is observed to increase gradually with the increase in the concentration of NiO beyond 0.6 mol %; this is an indicative of larger concentration of $Mo^{5+}O_3^-$ complexes in the glasses N_8 and N_{10}. The values of $g_\perp$ and g_{ll} from these spectra have been evaluated as 1.943 and 1.886; the structural disorder arising from the site-to-site fluctuations of the local surroundings of the paramagnetic Mo^{5+} ions can be accounted for the two components of the g values. The variation of NiO content seems to have no influence on the values of g even though the intensity of the signal is considerably affected. Further, the g values obtained for these glasses are found to be consistent with the reported values for many other glass systems (phosphate, borate, arsenate, etc.) containing molybdenum ions [36, 37]. The increase in the intensity and the half width $\Delta B_{1/2}$ of the signal with increase in the concentration of NiO (beyond 0.6 mol %) also supports the view point that in these glasses molybdenum ions exists largely in Mo^{5+} state.

In the IR spectra of $PbO–MoO_3–B_2O_3$: NiO glasses, the intensity of the bands due to more ordered BO_4 and MoO_4^{2-} tetrahedral units, is observed to be the highest for the glass N_6; with the increase of NiO content beyond 0.6 mol %, the intensity of the band due to BO_3 structural units is observed to build up at the expense of tetrahedral

bands. Further, the band due to ν_1 vibrational mode of MoO_4^{2-} tetrahedral units located at about 880 cm^{-1} (in the spectrum of the glass N_6) is observed to be shifted to the region of higher wavenumbers (915 cm^{-1}); in this region, the band due to partially isolated Mo–O bonds of strongly deformed MoO_6 groups is expected [38]. Similarly the ν_3 vibrational band of MoO_4^{2-} units observed at about 840 cm^{-1} in the spectrum of the glass N_6 is shifted towards the region of antisymmetric stretching vibrations of a Mo–$_{short}$O$_{long}$–Mo bridge associated with MoO_6 octahedral containing Mo=O bond (lower wavenumbers) [38]. These observations confirm that in the glasses containing NiO beyond 0.6 mol %, nickel ions mostly occupy octahedral positions, act as modifiers and are responsible for the increase in the degree of disorder in the glass network.

Among various electrical polarizations (viz., electronic, ionic, orientation and space charge), the space charge polarization depends on the purity and perfection of the glasses. With a gradual increase in the concentration of NiO in the glass matrix beyond 0.6 mol %, the values of ε', $\tan\delta$ and σ_{ac} are found to increase at any fixed frequency and temperature and the activation energy for a.c. conduction is observed to decrease. Obviously, this is because of an increasing concentration of octahedrally positioned Ni^{2+} and Mo^{5+} ions (evidenced from ESR and optical absorption measurements); these ions act as modifiers and generate bonding defects. The defects thus produced create easy pathways for the migration of charges that would build up space charge polarization leading to an increase in the dielectric parameters as observed [39]. When the concentration of NiO is increased up to 0.6 mol % in the glass matrix, the values of ε', $\tan\delta$ and σ_{ac} exhibit a decreasing trend (at any frequency and temperature) while the value of the activation energy for a.c. conduction exhibits an opposite trend; such a variation of these parameters may be ascribed to the presence of the cross linking of borate groups to form B–O–B and Pb–O–B bonds in the glass network as mentioned before. The presence of higher concentration of tetrahedral MoO_4^{2-} and NiO_4 units that take part network forming positions are also responsible for such low values of dielectric parameters in these samples.

The ascending values of $(\tan\delta)_{max}$, broadening of relaxation peaks and decrease in the value of activation energy for dipoles (Table 3) with increase in NiO concentration beyond 0.6 mol % in the glasses suggest an increase of freedom for dipoles to orient in the filed direction. This is also an indicative of decrease in the rigidity of the glass network. The observed dielectric relaxation effects may be attributed to the association of octahedrally positioned Ni^{2+} ions with a pair of any cationic vacancies in analogy with the mechanism-association of divalent positive ion with a pair of cationic vacancies – in conventional glasses, glass ceramics and crystals [40, 41].

If it is assumed that the electrical field in the glasses is the Lorenz field, the connection between the number N of the dipoles per unit volume, the electrical dipole moment μ and the low- and high-frequency electric permittivities ε_s and ε_∞ can be written according to the Clausius–Mossotti–Debye relation later modified by Guggenheim [42] as

$$\frac{\varepsilon_s - \varepsilon_\infty}{(\varepsilon_s + 2)(\varepsilon_\infty + 2)} T = \frac{4\pi N \mu^2}{27K} \tag{2}$$

Due to the fact that in the present glasses, ions and electric dipoles can be approximately regarded as mere points and the concentration of dipoles is not abnormally high, the applicability of the above equations for these glasses should be undoubted.

The quantity $N\mu^2$ in the right hand side of Eq. (2) represents the strength of dipoles. Substituting the values of ε_s and ε_∞, the quantity $4\pi N\mu^2/27K$ is calculated at 393 K for various concentrations of NiO and its dependence on the concentration of NiO is shown in the Fig. 11. The curve is observed to decrease up to 0.6 mol % of NiO and there after it is found to increase. Such a behaviour indicates an increase in the degree of spreading of relaxation times when the glasses are doped with NiO beyond 0.6 mol %. This result points out that in addition to Ni^{2+} ions, other type of dipoles also participating in relaxation effects. The other possibility is that Mo^{5+} (d^1) ions may form $Mo^{5+}O^{3-}$ complexes and may contribute to the relaxation effects [7, 35].

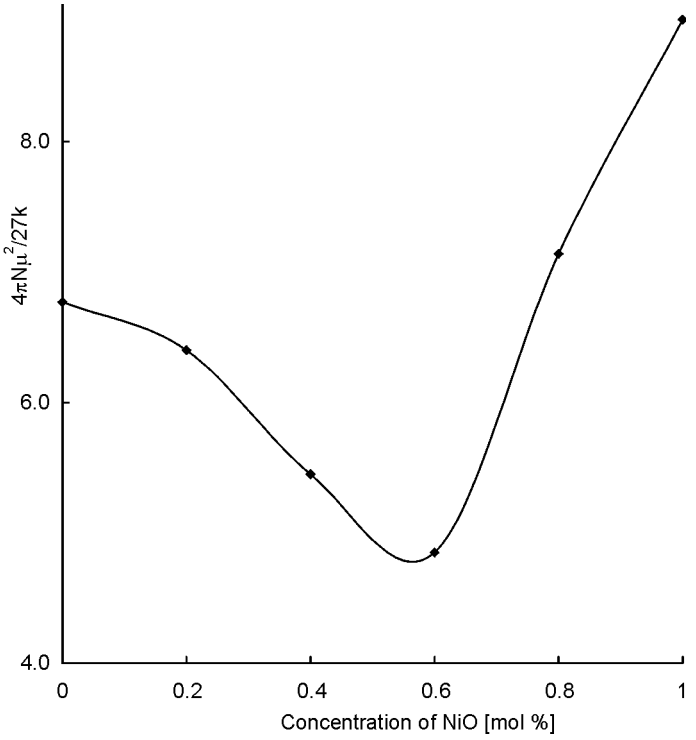

Fig. 11. Dependence of $4\pi N\mu^2/27k$ on concentration of NiO

In the plot $\log\sigma(\omega)$ vs. activation energy for conduction (in the high temperature region), a nearly linear relationship is observed (inset of Fig. 12); this observation

suggests that the conductivity enhancement is directly related to the thermally stimulated mobility of the charge carriers in the high temperature region [43]. Figure 12 represents the conductivity isotherms in function of NiO concentration; the curves pass through a minimum at approximately x = 0.6 mol %. The figure obviously suggests a kind of transition from predominantly electronic to ionic conductivity [44]. In the inset of the same figure, the activation energy for conduction is plotted in function of x. The plot is found to exhibit a maximum at x = 0.6 mol %.

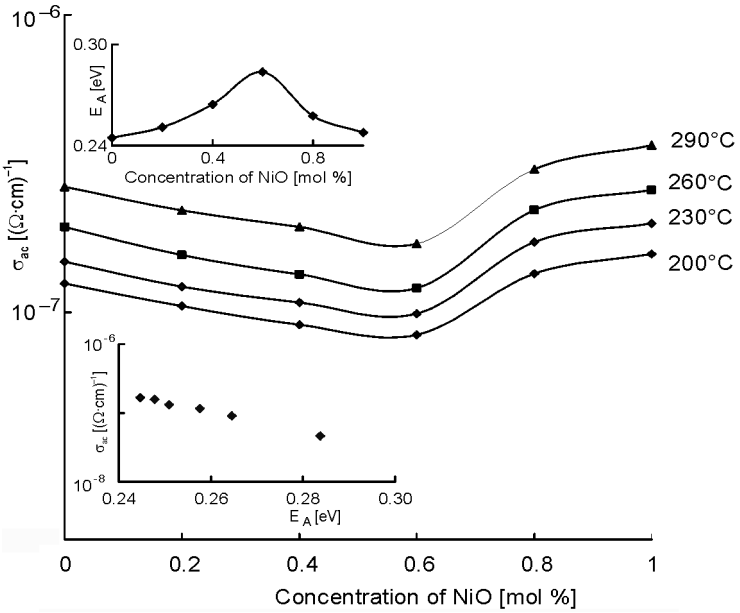

Fig. 12. Dependences of ac conductivity at 10 kHz on the concentration of NiO for $PbO–MoO_3–B_2O_3$ glasses. The upper inset shows dependence of activation energy on concentration of NiO, the lower one – dependence of ac conductivity on activation energy

Thus Figure 12 and its insets suggest the existence of two zones for conduction in the high temperature region viz., zone I, for $x < 0.6$ mol % and zone II for $x > 0.6$ mol %. In zone I, the electronic conduction seems to be dominant while in zone II, the ionic conductivity seems to be more significant. The possible explanation for this behaviour of conduction is as follows: With the entry of Ni^{2+} ions into the glass network, the electronic paths are progressively blocked causing an inhibition of the electronic current with a simultaneous increase in the ionic transport. The hopping polarons from $Mo^{5+} \longleftrightarrow Mo^{6+}$ responsible for conduction are attracted in pairs by the oppositely charged divalent nickel ions. This cation–polaron pairs move together as neutral entities. As expected, the migration of these pairs is not associated with any net displacement of the charge and thus does not contribute to electrical conductivity, as a result, a decrease in the conductivity up to 0.6 mol % of NiO.

The low temperature part of the conductivity (a nearly temperature independent part, as in the case of present glasses up to ca. 70 °C) can be explained based on the quantum mechanical tunnelling model [45] similar to many other glass systems reported recently from our laboratory [46–49]. The value of $N(E_F)$, i.e. the density of the defect energy states near the Fermi level, is evaluated using the equation [50]

$$\sigma(\omega) = \eta e^2 KT \left(N\left(E_F\right)\right)^2 \alpha^{-5} \omega \left(\ln\left(\frac{\nu_{ph}}{\omega}\right)\right)^4 \tag{3}$$

where η according to various authors is equal to: $\pi/3$ [45], $3.66\pi^2/6$ [51] or $\pi^4/96$ [52], for the frequency ($\omega = 2\pi r$) of 10^5 Hz at $T = 343$ K, taking $\alpha = 0.50$ $(Å)^{-1}$ (electronic wave function decay constant, obtained by plotting $\log\sigma_{ac}$ against R_i) and $\nu_{ph} \sim 5\times10^{12}$ Hz and in Table 4. The value of $N(E_F)$ is found to decrease with increasing concentration of NiO up to 0.6 mol % (indicating a decreasing disorder in the glass network, within this concentration range of NiO) and thereafter, it is observed to increase.

When a dielectric is placed in the electric field, the heat of dielectric loss is liberated. If the applied field is an alternating field, the specific dielectric loss, i.e., the loss per unit volume of the dielectric is given by [53]:

$$\rho_l = E^2 \omega \varepsilon' \varepsilon_0 \tan\delta \quad [W/m^3] \tag{4}$$

This equation indicates that the lower the values of $\varepsilon'\tan\delta$ of a glass at a given frequency, lower are the values of ρ_l. The dielectric breakdown strength is in fact inversely proportional to the specific dielectric loss represented by Eq. (4). Our observations on dielectric parameters of $PbO–B_2O_3–MoO_3$: NiO glasses, as mentioned earlier, indicate that the rate of increase of $\varepsilon'\tan\delta$ with temperature is gradually decreased with increase in the concentration of NiO up to 0.6 mol %. Thus the experiments on dielectric properties of $PbO–B_2O_3$-MoO_3: NiO glasses also reveal that there is an increase in the dielectric breakdown strength of the glasses with increase in the concentration of NiO up to 0.6 mol % indicating the high rigidity of the glass network.

5. Conclusions

The analysis of DTA results suggests that the glass forming ability is the highest for the glasses containing 0.6 mol % of NiO. The spectroscopic investigations point out that the nickel ions occupy both tetrahedral and octahedral positions in the glass network. The octahedral positions seem to be dominant when the content of NiO is higher than 0.6 mol % in the glass. The dielectric parameters, ε', $\tan\delta$ and σ_{ac} are found to decrease and the activation energy for ac conduction is found to increase with the increase in the concentration of NiO up to 0.6 mol%; a considerable increase in the ac conductivity is also observed when the concentration of NiO is increased from 0.6 to 1.0 mol % in the glass matrix. The analysis of dielectric relaxation effects exhibited

by these glasses indicates that there is a spreading of relaxation times. The conduction in the high-temperature region seems to be connected with both electronic and ionic; more specifically, up to 0.6 mol % of NiO, the electronic conduction seems to be dominant while in the higher concentration range, the ionic conduction seems to prevail.

References

[1] DEL NERY S.M., PONTUSUCHKA W.M., ISOTANI S., ROUSE C.G., Phys. Rev. B, 49 (1994), 3760.
[2] DA ROCHA M.S.F., PONTUSUCHKA W.M., BLAK A.R., J. Non-Cryst. Solids, 321 (2003), 29.
[3] MOGUS- MILANKOVIC A., SANTIC A., GAJOVIC A., DAY D E., J. Non-Cryst. Solids, 325 (2003), 76.
[4] SIMON S., NICULA A.C., J. Non-Cryst. Solids, 57 (1983), 23.
[5] LYNEH J.F., SAYER M., SEGEL S.L., ROSENBLATT G., J. Appl. Phys., 42 (1971), 2587.
[6] CHOWDARI B.V.R., TAN K.L., LING F., Solid State Ionics, 113 (1998), 711.
[7] BOUDLICH D., HADDAD M., KLIAVA J., J. Non-Cryst. Solids, 224 (1998),151.
[8] DAS B.B., AMBIKA R., Chem. Phys. Lett., 370 (2003), 670.
[9] CHOWDARI B.V.R., PRAMODA KUMARI P., Solid State Ionics, 113 (1998),665.
[10] BIH L., OMARI E.L., REAU J.M., YACOUBI A., NADIRI A., HADDAD M., Mater. Lett., 50 (2001), 308.
[11] ELKHOLY M.M., El-MALLAWANY R.A., Mater. Chem. Phys., 40 (1995), 63.
[12] MOGUS-MILANKOVIC A., SANTIC A., KARABULUT M., DAY D.E., J. Non-Cryst. Solids, 330 (2003), 128.
[13] GOVINARAJU G., BASKARAN N., SHAHI K., MANORAVI P., Solid State Ionics, 76 (1995), 47.
[14] ARDELEAN I., Mod Phys Lett, 16 (2001), 523.
[15] KUNDU T.K., CHAKRAVORTY D.K., J. Mater Res., 14 (1999), 1069.
[16] DESOKY El., MOHAMED S.M., KASHIF I., J. Mater. Sci. Mater. Electr., 10 (1999), 279.
[17] FAROUK H M., SANAD A., J. Mater. Sci. Mater. Electr., 6 (1995), 393.
[18] YOKOKAWA T., SHIBATA M., OOKAWA M., J. Non-Cryst. Solids, 190 (1995), 226.
[19] KASHIF I., FAROUK H., ALY S.A., J. Mater. Sci. Mater. Electr., 2 (1991), 216.
[20] KAMINSKII A.A., *Crystalline Lasers: Physical Processes and Operating Schemes*, CRC Press, Boca Raton, 1996.
[21] ZANNONI E., CAVALLI G., BETTINELLI M., J. Phys. Chem. Solids, 60 (1999), 449.
[22] NAGESWARA RAO P., RAGHAVAIAH B.V., KRISHNA RAO D., VEERAIAH N., J. Mater. Chem. Phys., 91 (2005), 381.
[23] SRINIVASA Reddy M., VEERAIAH N., J. Phys. Chem. Solids, 67 (2006), 789.
[24] AHMAD M.M., HOGARTH C.A., KHAN M.N., J. Mater. Sci., 19 (1984), 4041.
[25] KHALIFA F.A., EL BATAL H.A., AZOOZ A., Ind. J. Pure Appl. Phys., 36 (1998), 314.
[26] GOVINDARAJ G., BASKARAN N., SHAHI K., MANORAVI P., Solid State Ionics, 76 (1995), 47.
[27] MACHIDA N., ECKERT H., Solid State Ionics, 107 (1998), 255.
[28] MUTHUPARI S., PRABAKAR S., RAO K.J., J. Phys. Chem. Solids, 57 (1996), 553.
[29] SELVARAJ U., RAO K.J., Chem. Phys., 123 (1988a), 141; J. Non-Cryst. Solids, 104 (1988), 300.
[30] HUI-FEN WU., LIN CHUNG-CHENG, SHEN J.P., Non-Cryst. Solids, 209 (1997),76.
[31] RAO J.L., NARENDRA G.L., LAKSMAN S.V.J., Polyhedron, 9 (1990), 1475.
[32] RAO P.N., RAGHAVAIAH B.V., RAO D.K., VEERAIAH N., J. Lumin., 117 (2006), 53.
[33] GOLGSTEIN A., CHIRIAC V., BECHERESCU D., J. Non-Cryst. Solids, 92 (1987), 271.
[34] BOUDLICH D., HADDAD M., KLIAVA J., J. Non-Cryst. Solids, 224 (1998), 151.
[35] BIH L., OMARI El., HADDAD M., REAU J.M., BOUDLICH D., YACOUBI A., NADIRI A., Solid State Ionics, 132 (2000), 71.
[36] SRINIVASA RAO G., VEERAIAH N., J. Solid State Chem., 166 (2002), 104.

[37] HADDAD M., NADIRI A., BIYADI A., ARCHIDI M.E., FOLGADO J.V., BELTRAN-PORT D., J. Alloys Comp., 188 (1992), 161.
[38] IORDANOVA R., DIMITROV V., KLISSURSKI D., J. Non-Cryst. Solids, 231 (1998), 227.
[39] KRISHNA MOHAN N., SAMBASIVA RAO K., GANDHI Y., VEERAIAH N., Physica B, 6 (2006), 166.
[40] DURGA D. K., VEERAIAH N., J. Mater. Sci., 36 (2001), 5625.
[41] RADHA KRISHNAN S., SRINIVAS R.S., Phys. Rev. B, 14 (1976), 6967.
[42] BÖTTCHER C.J.F., BORDWIJK P., *Theory of Electrical Polarization* (Part II), Elsevier, New York 1978.
[43] EL-DAMARAWI G., J. Phys. Cond. Matter., 7 (1995), 1557.
[44] MONTANI R.A., FRECHERO M.A., Solid State Ionics, 158 (2003), 327.
[45] AUSTIN I.G., MOTT N.F., Adv. Phys., 18 (1969), 657.
[46] NAGA RAJU G., SRINIVASA RAO N., VEERAIAH N., Physica B, 373 (2006), 297.
[47] VENKATESWARA RAO G., VEERAIAH N., Phys. Chem. Glasses, 43 (2002), 205.
[48] SAHAYA BASKARAN G., LITTLE FLOWER G., KRISHNA RAO D., VEERAIAH N., J. Alloys Comp., 431 (2007), 303.
[49] RAO A.V., LAXMIKANTH C., VEERAIAH N., J. Phys. Chem. Solids, 67 (2007), 2263.
[50] ELLIOT S.R., *Physics of Amorphous Materials*, Longman, Essex, 1990.
[51] BUTCHER P., HYDEN K.J., Phil. Mag., 36 (1997), 657.
[52] POLLAK M., Phil. Mag., 23 (1971), 579.
[53] TAREEV B., *Physics of Dielectric Materials*, Mir, Moscow, 1979.

Received 18 May 2007
Revised 28 August 2007